

Long-term effects of main-body's obliquity on satellite formation perturbed by third-body gravity in elliptical and inclined orbit

Majid Bakhtiari¹, Kamran Daneshjou¹ and Mahdi Fakoore²

¹ Department of Mechanical Engineering, Iran University of Science and Technology, Narmak, Tehran 16844, Iran; kjoo@iust.ac.ir

² Department of Aerospace Engineering, Faculty of New Sciences and Technologies, University of Tehran, Tehran 4399-55941, Iran

Received 2016 October 13; accepted 2016 December 14

Abstract A new non-simplified model of formation flying is derived in the presence of an oblate main-body and third-body perturbation. In the proposed model, considering the perturbation of the third-body in an inclined orbit, the effect of obliquity (axial tilt) of the main-body is becoming important and has been propounded in the absolute motion of a reference satellite and the relative motion of a follower satellite. From a new point of view, J_2 perturbed relative motion equations and considering a disturbing body in an elliptic inclined three dimensional orbit, are derived using Lagrangian mechanics based on accurate introduced perturbed reference satellite motion. To validate the accuracy of the model presented in this study, an auxiliary model was constructed as the Main-body Center based Relative Motion (MCRM) model. Finally, the importance of the main-body's obliquity is demonstrated by several examples related to the Earth-Moon system in relative motion and lunar satellite formation keeping. The main-body's obliquity has a remarkable effect on formation keeping in the examined in-track and projected circular orbit (PCO) formations.

Key words: space vehicles — celestial mechanics — Moon — planets and satellites — formation — obliquity

1 INTRODUCTION

In recent years, formation flying as a key component of future space missions has become more and more attractive for researchers. Furthermore, derivation of the relative motion equations has a special importance for analyzing new space missions (Yang et al. 2015; Zeng et al. 2015). These equations were established primarily based on Keplerian circular orbits. Efforts were made to derive the equations for non-circular and perturbed orbits. Also, researchers have tried to obtain more accurate equations with consideration of zonal harmonics force (Casotto 2016), atmosphere drag (Gaias et al. 2015) and creating variations in reference satellite orbit characteristics (Chu et al. 2015).

For long-term missions of formation flying, satellite motion is affected by third-body perturbation and solar radiation pressure in high altitude orbits. Hence, in modern modeling and design of satellite formation (Gong

et al. 2011, 2009; Hu et al. 2016; Shahid & Kumar 2014), the perturbation force of third-body gravity and solar radiation are also considered in relative motion analysis.

The perturbation effect of a third-body on the absolute motion of a spacecraft in the inertial coordinate system has been extensively studied in the literature (Carvalho et al. 2010; Domingos et al. 2015, 2014, 2013; Lara et al. 2012). Using the average and double-average methods (Carvalho et al. 2010; Feng et al. 2015; Gomes & de Cássia Domingos 2015; Ma & Li 2013), investigation of prolonged flight in the presence of a disturbing-body is still an interesting research subject. In previous works, for simplification, the X-Y plane was introduced as a third-body's orbital plane instead of the equatorial plane of the main-body. Liu (Liu et al. 2012) was the first researcher who employed the double-average method to investigate the effect of a third-body's inclination angle on the absolute motion of a satellite.

Later, Ortore (Ortore et al. 2016) expanded the third-body gravity function as a Legendre polynomial up to second order, and analytically established the absolute motion equations of the satellite with consideration of an inclined third-body.

Nevertheless, the perturbation effect of a third-body on the relative motion of a spacecraft has attracted attention. Recently, for the first time Roscoe (Roscoe et al. 2013) has been able to analytically obtain the perturbation effects of the Moon on satellite formation, by using the model introduced by Bertachini de Almeida Prado (2003) without consideration of obliquity. An overall review of the literature shows that there are only a handful of papers on the modeling of satellites' relative motion in the presence of a third-body.

As can be found from the above literature, relative motion equations have not been solved exactly with consideration of third-body gravity and obliquity effects of a main-body. Also, in most of the previous works, the reference orbit perturbation has been ignored, which causes significant errors in long time flight. Also, it is demonstrated that the extension of the chaotic zone clearly depends on the value of obliquity and axial tilt can lead to large variation of orbit eccentricity (Liu et al. 2012). Furthermore, the amount of obliquity effects cannot be ignored for planets in the solar system. So, the purpose of this paper is to clarify the main-body's obliquity effects on relative motion and formation design.

To derive the near/far distance formation flying model, a new approach is employed to drive the non-simplified motion equations of the reference satellite in the presence of a third-body based on six hybrid elements. The comparison of absolute motion with previous models indicates that the proposed model has very good accuracy in long-duration flights. In the next step, by applying Lagrangian mechanics, the new exact relative motion equations have been extracted with consideration of third-body gravity in a three-dimensional orbit with an oblate main-body. To confirm the accuracy of the presented relative motion model, a model called the Main-body Center based Relative Motion (MCRM) model has been introduced. Finally, the effect of the main-body's axial tilt on two kinds of satellite formation (in-track and projected circular orbit (PCO)) is investigated.

2 THE DYNAMIC MODEL OF RELATIVE MOTION

The system studied in this work consists of four masses: a main-body with mass M , a perturbing-body with mass m' , reference satellite m and follower satellite m_j . The configuration of this system has been depicted in

Figure 1. Two coordinate systems have been used here. One, the main coordinate system ($OXYZ$), has its origin O attached to the center of mass of the main-body. The XY plane of this system coincides with the equatorial plane of the main-body and its Z -axis is towards the north pole of the main-body (Curtis 2013).

The other coordinate system is the Local-Vertical Local-Horizontal (LVLH) frame, whose origin is at the centroid of the reference satellite. This rotating frame generally rotates about the z -axis. By applying perturbation forces, it will experience another rotation around the x -axis. It should be mentioned that the LVLH system will not experience any rotation relative to the along-track direction. In this coordinate system, the x -axis (radial direction) is directed from the main-body center towards the reference satellite, and the z -axis (cross-track) is normal to the orbital plane of the reference satellite (Vallado 2001). Also, the y -axis (along-track) completes the LVLH coordinate system.

The angular rotational velocity of the LVLH frame is as follows

$$\boldsymbol{\omega} = \omega_x \mathbf{x} + \omega_y \mathbf{y} + \omega_z \mathbf{z}. \quad (1)$$

In the above equation, ω_x and ω_z are the steering rate and orbital rate of the orbital plane, respectively. Based on the orbital elements of the reference spacecraft, they are expressed as (Xu & Wang 2008)

$$\omega_x = \dot{i}c_\theta + \dot{\Omega}s_\theta s_i, \quad (2)$$

$$\omega_z = \dot{\theta} + \dot{\Omega}c_i, \quad (3)$$

where c_* and s_* represent $\cos(*)$ and $\sin(*)$ respectively. Also, i , θ and Ω represent inclination, argument of latitude and the right ascension of ascending node, respectively. The derivatives of these unit vectors are obtained as follows

$$\dot{\mathbf{x}} = \boldsymbol{\omega} \times \mathbf{x} = \omega_z \mathbf{y}, \quad (4)$$

$$\dot{\mathbf{y}} = \boldsymbol{\omega} \times \mathbf{y} = \omega_x \mathbf{x}, \quad (5)$$

$$\dot{\mathbf{z}} = \boldsymbol{\omega} \times \mathbf{z} = -\omega_x \mathbf{y}, \quad (6)$$

$$\mathbf{x} = \frac{\mathbf{r}}{|\mathbf{r}|}, \quad \mathbf{z} = \frac{\mathbf{h}}{|\mathbf{h}|}, \quad \mathbf{y} = \mathbf{z} \times \mathbf{x}. \quad (7)$$

Also, based on the orbital elements of the reference satellite, the angular velocity component about the y -axis is equal to zero (Kechichian 1998).

$$\omega_y = -\dot{i}s_\theta + \dot{\Omega}c_\theta s_i = 0. \quad (8)$$

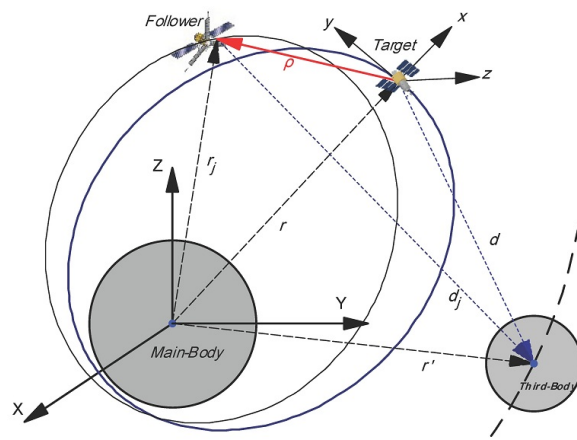


Fig. 1 Schematic diagram of the main-body centered coordinate system and relative frame attached to a center of reference satellite in the presence of an inclined perturbing-body.

2.1 Perturbed Reference Satellite Motion

In this work, the relative motion equations without simplification are defined on the basis of a perturbed reference orbit with regard to a disturbing-body in an inclined orbit as well as oblate main-body. Therefore, it is necessary to first derive the perturbed motion equations of the reference satellite.

It is assumed that the reference and follower satellites are orbiting around the main-body, with hybrid orbital elements $(r, v_x, i, h, \theta, \Omega)$ and $(r_j, v_{xj}, i_j, h_j, \theta_j, \Omega_j)$, respectively. Also, the third-body is in a Keplerian orbit with semimajor axis a' , eccentricity e' , inclination i' , argument of perigee ω' , argument of latitude θ' and right ascension of ascending

node Ω' (Xu et al. 2012). Based on the theory of celestial mechanics, the potential function due to a third-body perturbation is expressed as follows (Liu et al. 2012)

$$W' = \mu' \left(\frac{1}{d} - \frac{1}{r'^3} \mathbf{r} \cdot \mathbf{r}' \right), \quad (9)$$

where μ' is the perturbing-body gravitational constant, $r' = r'_x x + r'_y y + r'_z z$ is the vector connecting the centers of the main-body and third-body in the LVLH frame and $d = r' - r$ is the vector from the reference satellite toward the third-body center. That can be defined as follows

$$d = \sqrt{(r'_x - r)^2 + r'^2_y + r'^2_z}. \quad (10)$$

The gradient of the potential function of the perturbing-body is given as

$$\nabla W' = \left(-\frac{\mu'}{d^3} \right) \mathbf{r} + \left(\frac{\mu'}{r'^3} - \frac{\mu'}{d^3} \right) \mathbf{r}', \quad (11)$$

where the main-body is assumed to be an oblate body with zonal harmonic J_2 . Furthermore the gradient of the potential function of the main-body will be

$$\nabla W = \left(\frac{\mu}{r^3} + \frac{k_{J_2}}{r^5} (1 - 5s_\varphi^2) \right) \mathbf{r} + \frac{2k_{J_2}s_\varphi}{r^4} \mathbf{z}, \quad (12)$$

where $k_{J_2} = 3\mu J_2 R_e^2 / 2$ and $Z = s_i s_\theta x + s_i c_\theta y + c_i z$ as well as $s_\varphi = s_i s_\theta$. To obtain the gradient of the potential function applied on the reference satellite, it is necessary to express the position, velocity and acceleration vectors of the reference satellite in the LVLH frame. Thus, we have (Xu et al. 2012):

$$\mathbf{r} = r \mathbf{x}, \quad (13)$$

$$\dot{\mathbf{r}} = \mathbf{V} = v_x \mathbf{x} + \frac{\mathbf{h}}{r} \mathbf{y}, \quad (14)$$

$$\ddot{\mathbf{r}} = \left(v_x - \frac{h^2}{r^3} \right) \mathbf{x} + \frac{\dot{h}}{r} \mathbf{y} + \omega_x \frac{h}{r} \mathbf{z}. \quad (15)$$

In the above equations, h is the angular momentum, which is defined as $h = |\mathbf{r} \times \dot{\mathbf{r}}|$. By using the relation between the unit vectors $\mathbf{r} = \mathbf{x}$, $\mathbf{r} = [r \ 0 \ 0]^T$, $\mathbf{r}' = [r'_x \ r'_y \ r'_z]^T$ and a summation of Equations (11) and (12), the gradient of the potential function applied on the reference satellite is expressed in the LVLH frame as follows

$$\begin{aligned} \nabla W = & \left[\frac{\mu}{r^2} + \frac{k_{J2}}{r^4} (1 - 3s_i^2 s_\theta^2) - \frac{\mu'}{d^3} + \left(\frac{\mu'}{r'^3} - \frac{\mu'}{d^3} \right) r'_x \right] \mathbf{x} + \left[\frac{k_{J2}}{r^4} s_i^2 s_{2\theta} + \left(\frac{\mu'}{r'^3} - \frac{\mu'}{d^3} \right) r'_y \right] \mathbf{y} \\ & + \left[\frac{k_{J2}}{r^4} s_{2i} s_\theta + \left(\frac{\mu'}{r'^3} - \frac{\mu'}{d^3} \right) r'_z \right] \mathbf{z}. \end{aligned} \quad (16)$$

Now by employing the relation $\ddot{\mathbf{r}} = -\nabla W$ and by combining Equations (15) and (16), after some manipulations, the motion equations of the reference spacecraft in the presence of inclined third-body gravity and J_2 perturbation can be derived as in Equations (17)–(22).

$$\dot{r} = v_x, \quad (17)$$

$$v_x = -\frac{\mu}{r^2} + \frac{h^2}{r^3} - \mu' \left(\frac{1}{r'^3} - \frac{1}{d^3} \right) r'_x - \frac{\mu_m}{d^3} r - \frac{k_{J2}}{r^4} (1 - 3s_i^2 s_\theta^2), \quad (18)$$

$$\dot{h} = -\mu' \left(\frac{1}{r'^3} - \frac{1}{d^3} \right) r'_y r - \frac{k_{J2}}{r^4 s_i^2} s_{2\theta}, \quad (19)$$

$$\dot{\theta} = \frac{h}{r^2} + \frac{2k_{J2}}{hr^3} c_i^2 s_{2\theta} + \frac{rc_i s_\theta}{hs_i} \mu' \left(\frac{1}{r'^3} - \frac{1}{d^3} \right) r'_z, \quad (20)$$

$$i = -\frac{r}{h} c_\theta \mu' \left(\frac{1}{r'^3} - \frac{1}{d^3} \right) r'_z - \frac{k_{J2}}{2hr^3} s_{2i}^2 s_{2\theta}, \quad (21)$$

$$\dot{\Omega} = -\frac{r}{h} \frac{s_\theta}{s_i} \mu' \left(\frac{1}{r'^3} - \frac{1}{d^3} \right) r'_z - \frac{2k_{J2}}{hr^3} s_\theta^2 c_i. \quad (22)$$

The motion equations of the reference satellite are extracted without any simplification with six hybrid orbital elements. The motion equations obtained for the reference satellite are independent of Ω . Thus, it can be analyzed by using the five equations given by Equations (17)–(21). Also, this equation considers the perturbing-body inclination that is important for long-term motion evaluation.

Furthermore, the orbital rate ω_z is equal to (Wei et al. 2013)

$$\omega_z = \frac{h}{r^2}. \quad (23)$$

Also, by using Equations (15) and (16), the steering rate of the orbital plane will be determined as

$$\omega_x = -\frac{k_{J2}}{hr^3} s_\theta s_{2i} - \mu' \left(\frac{1}{r'^3} - \frac{1}{d^3} \right) r'_z \frac{r}{h}. \quad (24)$$

Then, by using Equations (23), (24) and (19), the expressions related to the time derivative of the rotation components of the LVLH system relative to the main coordinate system can be derived as follows:

$$\begin{aligned} \alpha_x = \dot{\omega}_x = & -\mu' \frac{r}{h} \left(\frac{1}{r'^3} - \frac{1}{d^3} \right) \left(\frac{\dot{r}}{r} - \frac{\dot{h}}{h} \right) r'_z + 3 \frac{r}{h} \mu' \left(\frac{\dot{r}'}{r'^4} - \frac{\dot{d}}{d^4} \right) r'_z \\ & + \frac{k_{J2}}{h^2 r^6} \left(-8k_{J2} s_i^3 s_\theta^2 c_i c_\theta + 3hr^2 v_x s_\theta s_{2i} - h^2 r c_\theta s_{2i} \right). \end{aligned} \quad (25)$$

$$\alpha_z = \dot{\omega}_z = -\frac{k_{J2}}{r^5} s_{2\theta} s_i^2 - \frac{2v_x h}{r^3} - \frac{\mu'}{r} \left(\frac{1}{r'^3} - \frac{1}{d^3} \right) r'_y, \quad (26)$$

where

$$\dot{d} = [(r'_x - \dot{r}) + r'_y + r'_z]. \quad (27)$$

2.2 Dynamics of Perturbed Relative Motion

In the second step, the motion equations of the follower satellite relative to the reference satellite should be obtained. For this purpose, Lagrange's equations are used to derive the relative motion model for the j th satellite.

In general, by setting the Lagrangian equal to the difference between the kinetic and potential energies of the j th satellite ($L_j = K_j - U_j$), Lagrange's equation for deriving the relative motion model can be expressed as Equation (28) (Bosanac et al. 2016)

$$\frac{d}{dt} \left(\frac{\partial K_j}{\partial \dot{q}_n} \right) - \frac{\partial K_j}{\partial q_n} + \frac{\partial U_j}{\partial q_n} = Q_{n^j}, \quad (28)$$

in which $q_j = [x_j \ y_j \ z_j]^T$ is the generalized displacement and $\dot{q}_j = [\dot{x}_j \ \dot{y}_j \ \dot{z}_j]^T$ is the generalized velocity. Also, Q_{n^j} is the sum of the non-conservative forces applied on the j th satellite. Here, Q_n^j denotes the control force applied on the follower satellite. Now, by precisely computing the potential and kinetic functions, the relative dynamic equations for the motion of the j th satellite in the LVLH system can be derived.

2.2.1 Kinetic energy

The position vector \mathbf{r}_j of the j th satellite in the LVLH frame is

$$\mathbf{r}_j = (r + x_j) \mathbf{x} + y_j \mathbf{y} + z_j \mathbf{z}. \quad (29)$$

The velocity vector \mathbf{V}_j is obtained by taking the derivative of Equation (29) and substituting Equations (4)–(6)

$$\dot{\mathbf{r}}_j = \mathbf{V} = (v_x - \dot{x}_j - y_j \omega_z) \mathbf{x} - \left(\frac{h}{r} + \dot{y}_j + x_j \omega_z - z_j \omega_x \right) \mathbf{y} + (\dot{z}_j + y_j \omega_x) \mathbf{z}. \quad (30)$$

The kinetic energy (per unit mass) for the j th satellite is obtained in Equation (31)

$$K_j = \frac{1}{2} \dot{\mathbf{r}}_j^T \dot{\mathbf{r}}_j = \frac{1}{2} \left[(v_x - \dot{x}_j - y_j \omega_z)^2 + \left(\frac{h}{r} + \dot{y}_j + x_j \omega_z \right)^2 + (\dot{z}_j + y_j \omega_x)^2 \right]. \quad (31)$$

Substituting Equation (31) into the first two terms of Lagrange's equation (Eq. 28) gives

$$\begin{bmatrix} \ddot{x}_j - 2\dot{y}_j \omega_z - x_j \omega_z^2 - y_j \alpha_z + z_j \omega_x \omega_z - r (\omega_z)^2 + (\dot{v}_x) \\ \ddot{y}_j - 2\dot{x}_j \omega_z - 2\dot{z}_j \omega_x + x_j \alpha_z - y_j \omega_z^2 - y_j \omega_x^2 - z_j \alpha_x + 2v_x (\omega_z) + r (\alpha_z) \\ \ddot{z}_j + 2\dot{x}_j \omega_x + x_j \omega_x \omega_z + y_j \alpha_x - z_j \omega_x^2 - r (\omega_z \omega_x) \end{bmatrix}. \quad (32)$$

By using Equations (18), (23), (24) and (26) and substituting into the expression within the parenthesis in Equation (32), the following expression is obtained

$$\frac{d}{dt} \left(\frac{\partial K_j}{\partial \dot{q}_n} \right) - \frac{\partial K_j}{\partial q_n} = \begin{bmatrix} \ddot{x}_j - 2\dot{y}_j \omega_z - x_j \omega_z^2 - y_j \alpha_z + z_j \omega_x \omega_z - r y^2 - \frac{\mu}{d^3} r \mu' \left(\frac{1}{r'^3} - \frac{1}{d^3} \right) r'_x - \chi s_i s_\theta \\ \ddot{y}_j - 2\dot{x}_j \omega_z - 2\dot{z}_j \omega_x + x_j \alpha_z - y_j \omega_z^2 - y_j \omega_x^2 - z_j \alpha_x - \mu' \left(\frac{1}{r'^3} - \frac{1}{d^3} \right) r'_y - \chi s_i c_\theta \\ \ddot{z}_j + 2\dot{x}_j \omega_x + x_j \omega_x \omega_z + y_j \alpha_x - z_j \omega_x^2 - \mu' \left(\frac{1}{r'^3} - \frac{1}{d^3} \right) r'_z - \chi c_i \end{bmatrix}, \quad (33)$$

where

$$\chi = \frac{2k_{J2}}{r^4} s_\theta s_i, \quad (34)$$

$$\gamma^2 = \frac{\mu}{r^3} + \frac{k_{J2}}{r^5} - \frac{5k_{J2}}{r^5} s_\theta^2 s_i^2. \quad (35)$$

2.2.2 Potential energy

The applied gravitational potential energy on the j th satellite, due to the gravitational fields of the main-body and third-body (similar to Eq. (9)), is expressed as follows

$$U_j = \frac{\mu}{r_j} - \frac{k_{J2} r_{jz}^2}{3r_j^3} + \frac{k_{J2}}{r_j^5} - \mu' \left(\frac{1}{d_j} - \frac{1}{r'^3} \mathbf{r}_j \cdot \mathbf{r}' \right), \quad (36)$$

where r_j and $r_j Z$ are given as

$$r_j = \sqrt{(r + x_j)^2 + y_j^2 + z_j^2}, \quad (37)$$

$$r_{jz} = \mathbf{r}_j \cdot \hat{\mathbf{Z}}. \quad (38)$$

Thus, with regard to Equation (28) and using Equation (36) we will have

$$\frac{\partial U_j}{\partial q_j} = \begin{bmatrix} \gamma_j^2 - 2(r + x_j) + \chi_j s_i s_\theta + \mu' \left(\frac{1}{r'^3} - \frac{1}{d_j^3} \right) r'_x + \frac{\mu' (r + r'_x)}{d_j^3} \\ \gamma_j^2 y_j + \chi_j s_i c_\theta + \mu' \left(\frac{1}{r'^3} - \frac{1}{d_j^3} \right) y_m + \frac{\mu' r'_x}{d_j^3} \\ \gamma_j^2 z_j + \chi_j c_i + \mu' \left(\frac{1}{r'^3} - \frac{1}{d_j^3} \right) z_m + \frac{\mu' r'_z}{d_j^3} \end{bmatrix}, \quad (39)$$

where

$$\chi_j = \frac{2k_{J2}}{r_j^5} r_{jz}, \quad (40)$$

$$\gamma_j^2 = \frac{\mu}{r_j^3} + \frac{k_{J2}}{r_j^5} - \frac{5k_{J2} r_j Z^2}{r_j^7}, \quad (41)$$

$$d_j = |\mathbf{r}' - \mathbf{r}_j| = \sqrt{(r'_x - (r + x_j))^2 + (r'_y - y_j)^2 + (r'_z - z_j)^2}. \quad (42)$$

Now, by using Equations (33), (39) and (28) and considering thrust forces to be non-conservative, the motion equations of the j th satellite relative to the reference satellite can be obtained as:

$$\begin{aligned} \ddot{x}_j = 2\dot{y}_j \omega_z - x_j \gamma_j^2 + x_j \omega_z^2 + y_j \alpha_z - z_j \omega_x \omega_z + \frac{\mu'}{d^3} r - r'_x \mu' \left(\frac{1}{d^3} - \frac{1}{d_j^3} \right) - \left(\frac{\mu}{r_j^3} + \frac{\mu'}{d_j^3} \right) (r + x_j) \\ - (\chi_j - \chi) s_\theta s_i - r (\gamma_j^2 - \gamma^2) + T_{xj}, \end{aligned} \quad (43)$$

$$\begin{aligned} \ddot{y}_j = -2\dot{x}_j \omega_z + 2\dot{z}_j \omega_x + y_j \gamma_j^2 - x_j \alpha_z + y_j (\omega_x^2 + \omega_z^2) - r'_y \mu' \left(\frac{1}{d^3} - \frac{1}{d_j^3} \right) - \left(\frac{\mu}{r_j^3} + \frac{\mu'}{d_j^3} \right) \\ y_j - (\chi_j - \chi) s_\theta s_i + T_{yj}, \end{aligned} \quad (44)$$

$$\ddot{z}_j = -2\dot{y}_j \omega_x - z_j \gamma_j^2 + z_j \omega_x^2 + y_j \alpha_x - x_j \omega_x \omega_z - r'_z \mu' \left(\frac{1}{d^3} - \frac{1}{d_j^3} \right) - \left(\frac{\mu}{r_j^3} + \frac{\mu'}{d_j^3} \right) z_j - (\chi_j - \chi) c_i + T_{zj}, \quad (45)$$

where T_{xj}, T_{yj}, T_{zj} are control force components on the j th spacecraft. Thus, the equations obtained for the relative motion of the satellites are derived without any simplification and, moreover, the J_2 perturbation and disturbing-body in an inclined elliptical orbit are considered. To analyze the relative motion of the controllable satellite, it is necessary to use Equations (43)–(45) together with Equations (17)–(22), so that the variations of reference satellite orbital elements are computed instantaneously and applied to the relative motion equations.

2.3 The Third-Body Motion in LVLH Frame

By using Equations (17)–(22) and (43)–(45), the reference and follower satellite motion as well as formation operation can be analyzed. For employing these equations, the displacement $[r'_x, r'_y, r'_z]$ and velocity $[\dot{r}'_x, \dot{r}'_y, \dot{r}'_z]$ components of a perturbing body in the LVLH frame must be known. To obtain these components, the following procedure is given:

1- The classical orbital elements of the third-body in an inclined elliptical orbit ($a', i', e', \omega', \Omega', f'$) are obtained based on Keplerian motion.

2- The position and velocity vectors of the third-body in the perifocal frame are provided using the perturbing-body's classical orbital elements by (Curtis 2013)

$$\bar{\mathbf{r}}' = \frac{h'}{\mu'} \frac{1}{1 + e' c_{f'}} (c_{f'} \mathbf{p} + s_{f'} \mathbf{q}), \quad (46)$$

$$\dot{\bar{\mathbf{r}}}' = \bar{\mathbf{v}}' = \frac{h'}{\mu'} [-c_{f'} \mathbf{p} + (e' + c_{f'}) \mathbf{q}], \quad (47)$$

where the unit vector along the \bar{x} -axis (the apse line in the perifocal frame) is denoted by \mathbf{p} . The \bar{y} -axis, with unit vector \mathbf{q} , lies along the 90° true anomaly to the \bar{x} -axis.

3- By applying transfer matrix and third-body orbital elements (Qi & Xu 2015), the position and velocity vectors of the third-body in the perifocal frame can transfer to the main-body frame as follows

$$\begin{bmatrix} c_{\omega'} c_{\Omega'} - s_{\omega'} c_{i'} s_{\Omega'} & -s_{\omega'} c_{\Omega'} - c_{\omega'} c_{i'} s_{\Omega'} & s_{\omega'} s_{\Omega'} \\ c_{\omega'} s_{\Omega'} + s_{\omega'} c_{i'} c_{\Omega'} & -s_{\omega'} s_{\Omega'} - c_{\omega'} c_{i'} c_{\Omega'} & -s_{i'} c_{\Omega'} \\ s_{\omega'} s_{i'} & c_{\omega'} s_{i'} & c_{i'} \end{bmatrix}, \quad (48)$$

$$\mathbf{r}'^E = Q_p^E \bar{\mathbf{r}}', \quad (49)$$

$$\mathbf{v}'^E = Q_p^E \bar{\mathbf{v}}'. \quad (50)$$

4- Now, by using the transfer matrix based on the orbital elements of the reference satellite (Alfriend et al. 2009), the position and velocity of the third-body in the LVLH coordinate system can be obtained.

$$\Phi_E^L = \begin{bmatrix} c_\theta c_\Omega - s_\theta c_i s_\Omega & c_\theta c_\Omega + s_\theta c_i c_\Omega & s_\theta s_i \\ -s_\theta c_\Omega - c_\theta s_i s_\Omega & -s_\theta s_\Omega - c_\theta c_i c_\Omega & c_\theta s_i \\ s_i s_\Omega & -s_i c_\Omega & c_i \end{bmatrix}, \quad (51)$$

$$\mathbf{r}' = \Phi_E^L \mathbf{r}'^E = [r'_x, r'_y, r'_z]^T, \quad (52)$$

$$\mathbf{v}' = \Phi_E^L \mathbf{v}'^E = [\dot{r}'_x, \dot{r}'_y, \dot{r}'_z]^T. \quad (53)$$

3 MAIN-BODY CENTERED BASED RELATIVE MOTION (MCRM) MODEL

To ascertain the validity and accuracy of the presented model, the structure of an MCRM model is constructed. To establish such a structure, the equations of the reference and follower satellite should be written in the main-body frame. The equations of motion of the reference satellite perturbed by the third body are given as

$$\ddot{\mathbf{R}} = -\frac{\mu}{R^3} \mathbf{R} + \nabla \left[-\frac{\mu}{R^3} J_2 R_e^2 P_2 \left(\frac{Z}{R} \right) \right] + \mu_m \left(\frac{\mathbf{D}}{D^3} - \frac{\mathbf{R}_m}{R_m^3} \right), \quad (54)$$

where \mathbf{R} is the satellite's position vector, \mathbf{R}' is the third-body's position vector and $\mathbf{D} = \mathbf{R}_m - \mathbf{R}$ is the vector connecting the centroid of the reference satellite to the disturbing body center in the main-body frame. Similarly, the perturbed j th follower motion in the main-body centered frame, with regards to the thrust force, can be expressed as follows

$$\ddot{\mathbf{R}}_j = -\frac{\mu}{R_j^3} \mathbf{R}_j + \nabla \left[-\frac{\mu}{R_j^3} J_2 R_e^2 P_2 \left(\frac{Z_j}{R_j} \right) \right] + \mu_m \left(\frac{\mathbf{D}_j}{D_j^3} - \frac{\mathbf{R}_m}{R_m^3} \right). \quad (55)$$

Now, by using Equations (54) and (55), the position and velocity of each satellite in the main-body coordinate system can be obtained. Finally, by subtracting the position and velocity components of the satellites, the relative position and velocity of the follower satellite will be obtained.

$$\boldsymbol{\rho} = [\Phi_I^L] \mathbf{R}_j - \mathbf{R}, \quad (56)$$

$$\dot{\boldsymbol{\rho}} = [\dot{\Phi}_I^L] \dot{\mathbf{R}} + [\Phi_I^L] \dot{\mathbf{R}} - \boldsymbol{\omega} \times \boldsymbol{\rho}. \quad (57)$$

To do this, the position $\mathbf{R}_j = [X_j \ Y_j \ Z_j]^T$ and velocity $\dot{\mathbf{R}}_j = [\dot{X}_j \ \dot{Y}_j \ \dot{Z}_j]^T$ of the follower satellite in the main-body centered coordinate system, as well as position $\mathbf{r} = [r \ 0 \ 0]^T$ and velocity $\dot{\mathbf{r}} = [v_x \ h/r \ 0]^T$ of the reference satellite in the LVLH frame, angular velocity vector of the reference orbit $\boldsymbol{\omega} = [\omega_x \ 0 \ \omega_z]^T$ and transfer matrix $[\Phi_I^L]$ at any moment, are required. The array of $[\Phi_I^L]$ is dependent on the reference orbital elements. This structure is explained in Figure 2.

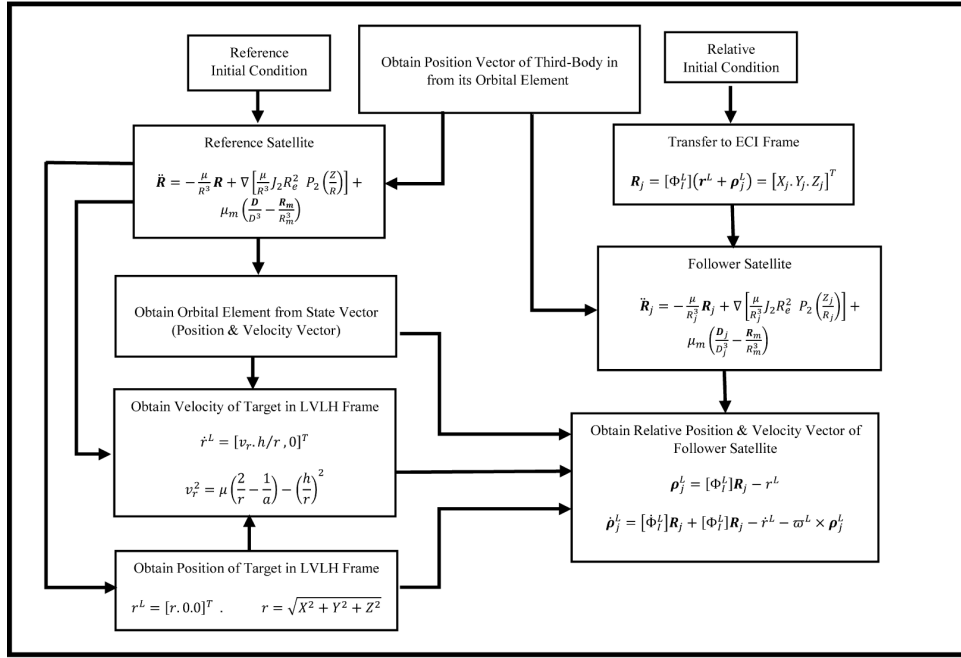


Fig. 2 Flowchart of the MCRM model.

4 RESULT ANALYSIS

In this section, several numerical simulations are performed to validate the presented model for both the reference satellite and the follower's relative motion. The model introduced by Liu et al. (2012) is used to validate the motion equations of the reference spacecraft (Eqs. (17)–(22)). The presented relative motion equations are also validated against the MCRM model which is produced in this study to fill the gap of available data. After verifying the presented model, the necessity for consideration of main-body's obliquity on relative motion and formation design will be investigated.

4.1 Earth-Moon System

As mentioned earlier, in this study, it is assumed that the Moon is the main-body and the reference satellite is orbiting around the Moon. These motions are perturbed by the Earth as a third-body. Also, contrary to the works of (Carvalho et al. 2011, 2010; Gong & Li 2015; Qi & Xu 2015) in which the inclination of the third-body has been ignored, here, the inclination of the perturbing-body is not considered to be zero (see Tresaco et al. (2016)). Also, no restriction has been employed in obtaining the equations or simulations. The motion of the reference spacecraft obtained in this study is validated against the results obtained by Liu et al. (2012) (with consideration of i' and the double averaged method), by similar

orbital parameters. Figure 3 and 4 illustrate the effect of the main-body's obliquity and difference between the double-averaging and the proposed exact solution.

In Figures 3 and 4, the exact proposed model of satellite motion by Equations (1)–(6) is compared with the double-average model (Liu et al. 2012) to show the accuracy of the model in long-time flight in the presence of a third-body perturbation. In Liu's work, some simplifications were considered to derive the motion equation of a satellite under inclined third body perturbation. Also, the only perturbing force that was considered in Liu's paper was the third body gravity effect of orbiting in a 6.68° inclined orbit. The third body perturbation force was inversely proportional to the distance between the third body and satellite, so that with distance decreasing between the third body and satellite, the perturbing force increased and had a significant effect on satellite motion. Based on the above-mentioned issues Liu's work had some simplification to include the influence of the Moon's gravity on the satellite motion equation. These simplifications cause an approximate value of lunar perturbation to be employed in the computation. Also, by decreasing the distance between the third body and the satellite, the error due to simplification offered by Liu's work became larger with more elapsed time.

In the next step, the relative motion of the follower spacecraft is validated against the presented MCRM model. The initial conditions of the reference and fol-

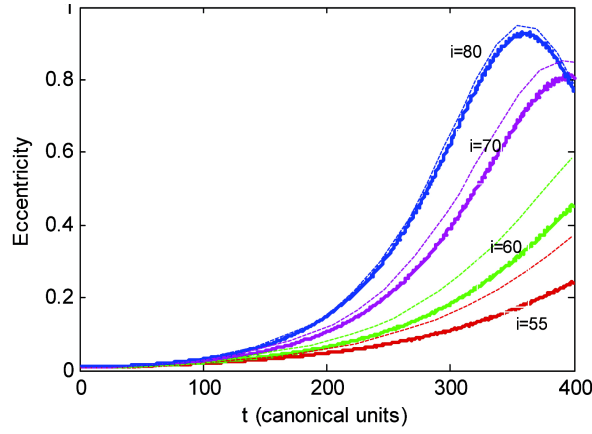


Fig. 3 Variation of eccentricity over 400 canonical time units (1737 days) for different initial inclinations, double-averaged model (Liu et al. 2012) (*dashed-lines*) and the proposed model (*solid-lines*).

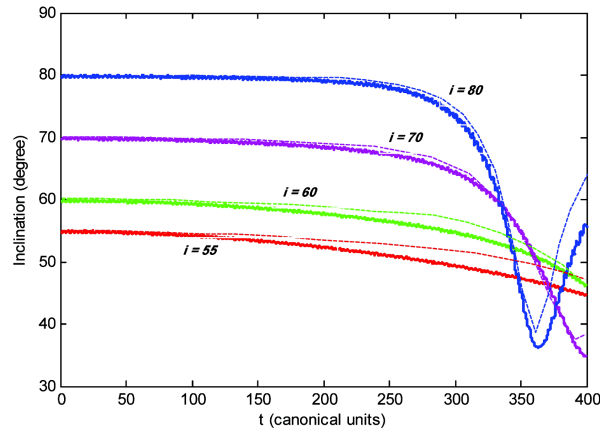


Fig. 4 Variation of inclination over 400 canonical time units (1737 days) for different initial inclinations, double-averaged model (Liu et al. 2012) (*dashed-lines*) and the proposed model (*solid-lines*).

lower spacecraft are presented in Equation (58):

$$\begin{aligned}
 a &= 6244 \text{ km}, e = 0.25, i = 35^\circ, \Omega = 41^\circ, \theta = 18^\circ, \\
 &\quad \omega = 30^\circ, \text{ for reference orbit} \\
 a &= 6239 \text{ km}, e = 0.21, i = 36^\circ, \Omega = 40^\circ, \theta = 20^\circ, \\
 &\quad \omega = 31^\circ, \text{ for follower A orbit} \\
 a &= 5998 \text{ km}, e = 0.10, i = 30^\circ, \Omega = 35^\circ, \theta = 10^\circ, \\
 &\quad \omega = 20^\circ \text{ for follower B orbit.}
 \end{aligned} \tag{58}$$

Also, by using Equations (56) and (57), the initial conditions for the relative motion of the follower spacecraft in the LVLH system are obtained.

As seen in Figures 5 and 6, the results obtained by the suggested model show a very good agreement with the MCRM model. It should be noted that in all simulations it was supposed that the third-body is in an elliptic inclined three-dimensional Keplerian orbit around

the main body with $a' = 386000 \text{ km}$, $e' = 0.05$, $i' = 6.68^\circ$, $\omega' = \Omega' = 0$.

4.2 Obliquity Effects on Relative Motion

In this section, several simulations have been made to investigate the main-body's obliquity effects with different initial conditions for followers in specific cases of formation flying. For this purpose, first, the lunar orbiter is considered with the following orbital elements that orbit around a spherical Moon (neglecting the J_2 zonal harmonic of the Moon being equal to 2.0320×10^{-4})

$$\begin{aligned}
 a &= 5844 \text{ km}, e = 0.10, i = 20^\circ, \Omega = 15^\circ, \\
 &\quad \theta = 30^\circ, \omega = 30^\circ, \text{ for reference orbit.}
 \end{aligned} \tag{59}$$

For simulation of different scenarios, the follower orbital element is assumed to be the same as Equation (59) with consideration of some variation in these orbital elements. Accordingly, the initial conditions of follower satellites

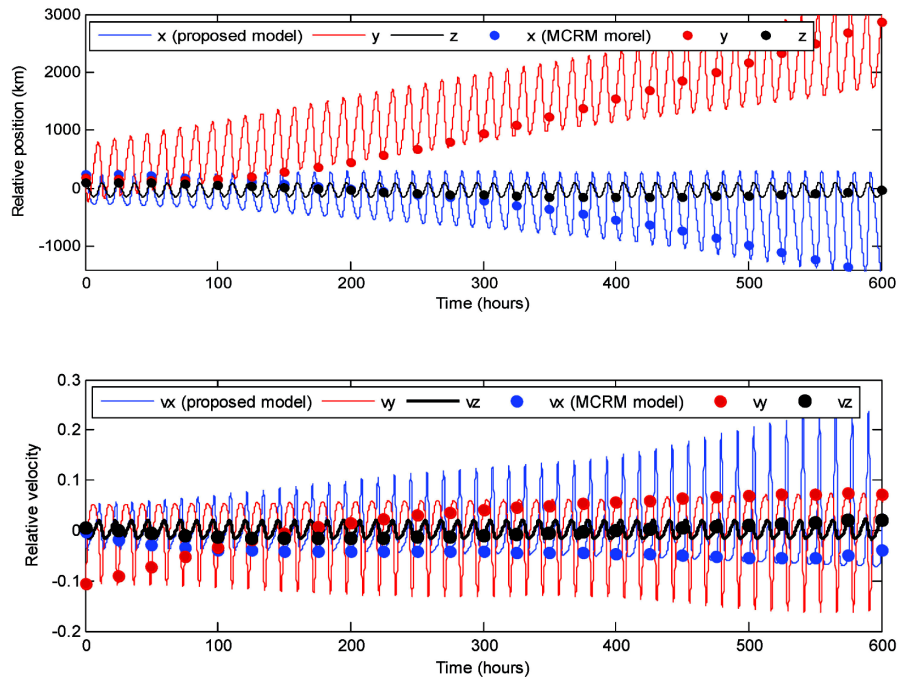


Fig. 5 The relative position and velocity for follower A, the MCRM model (*bullets*) and the presented model (*lines*).

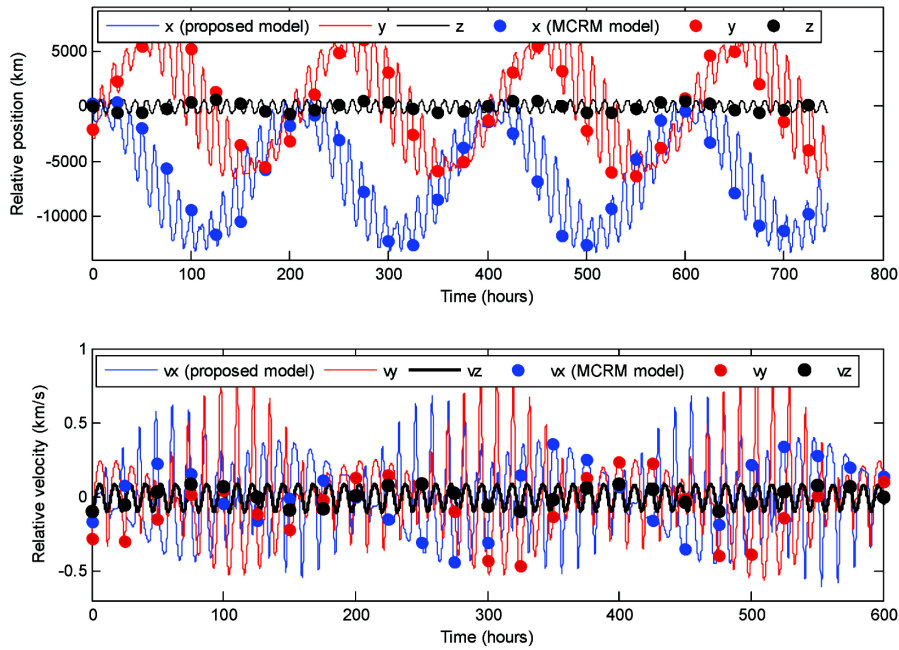


Fig. 6 The relative position and velocity for follower B, the MCRM model (*bullets*) and the presented model (*lines*).

are given in Table 1 with regard to above-mentioned variations. It should be noted that these initial conditions are obtained using the variation of each orbital element of the reference satellite and by employing Equations (56) and (57).

Figure 7 depicts the obliquity effects of the Moon on the position and velocity components of the follower. It shows that a significant deviation is produced in long-term prediction of relative motion, despite low axial tilt of the Moon. As can be found from Figure 7, when the ar-

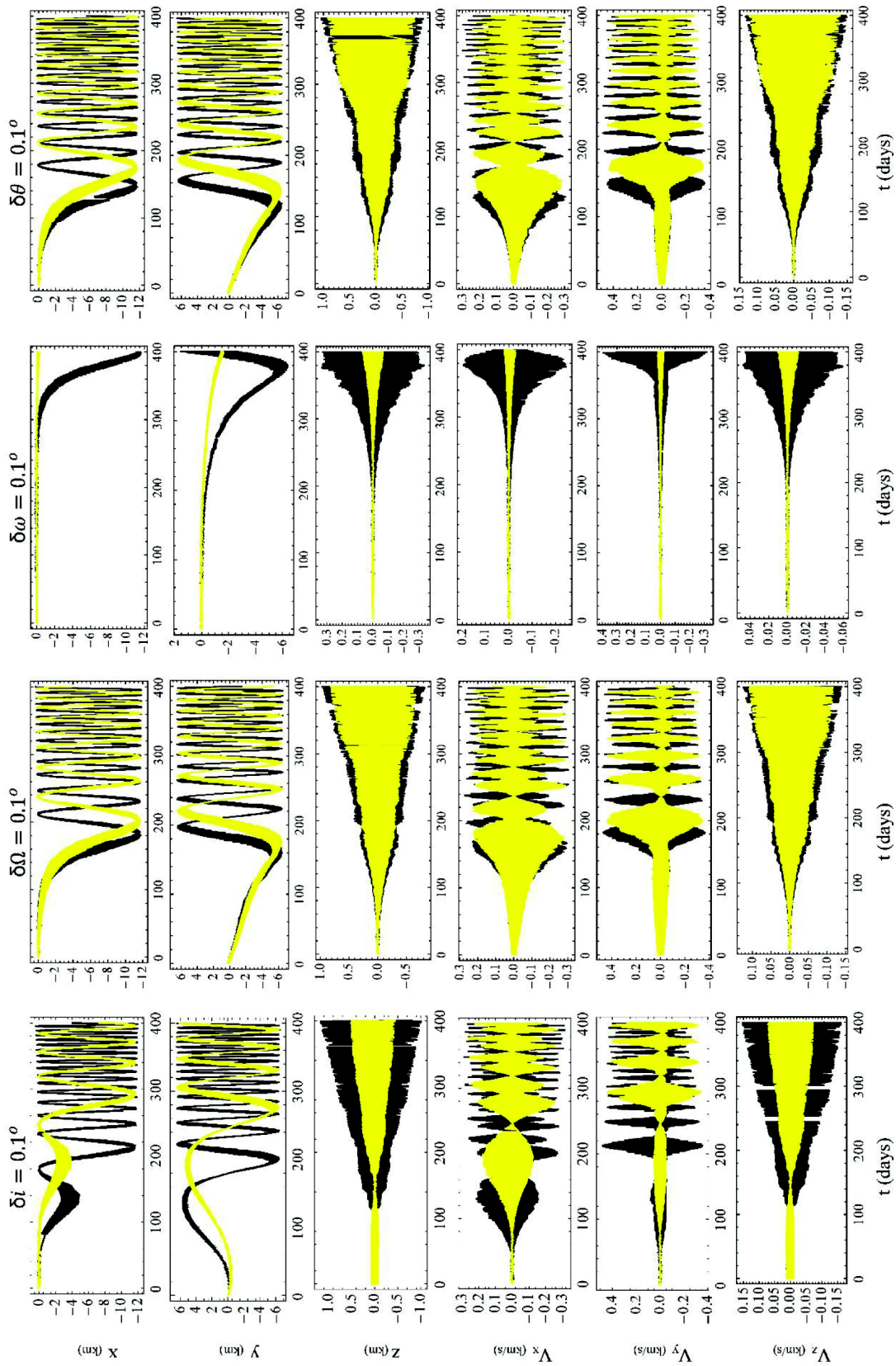


Fig. 7 The position and velocity components of the follower satellite considering the obliquity of the Moon (yellow lines) and neglecting the obliquity effect (black lines) effect.

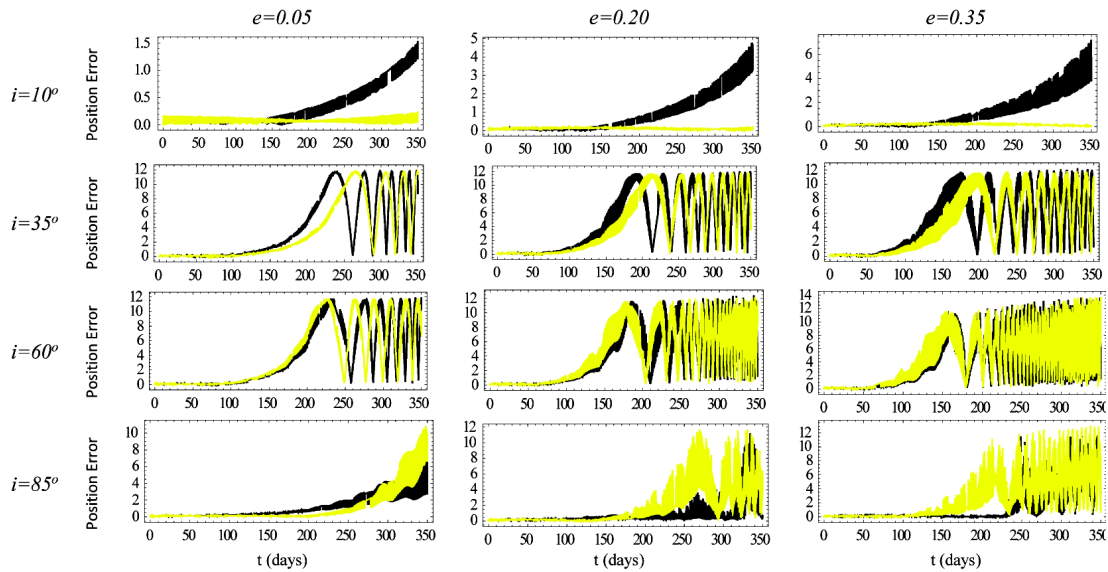


Fig. 8 The position of the follower satellite in the LVLH frame in different inclinations and eccentricities of the reference orbit with constant perigee. (Yellow and black correspond to the simulation with consideration of lunar axial tilt and with ignorance of obliquity, respectively.)

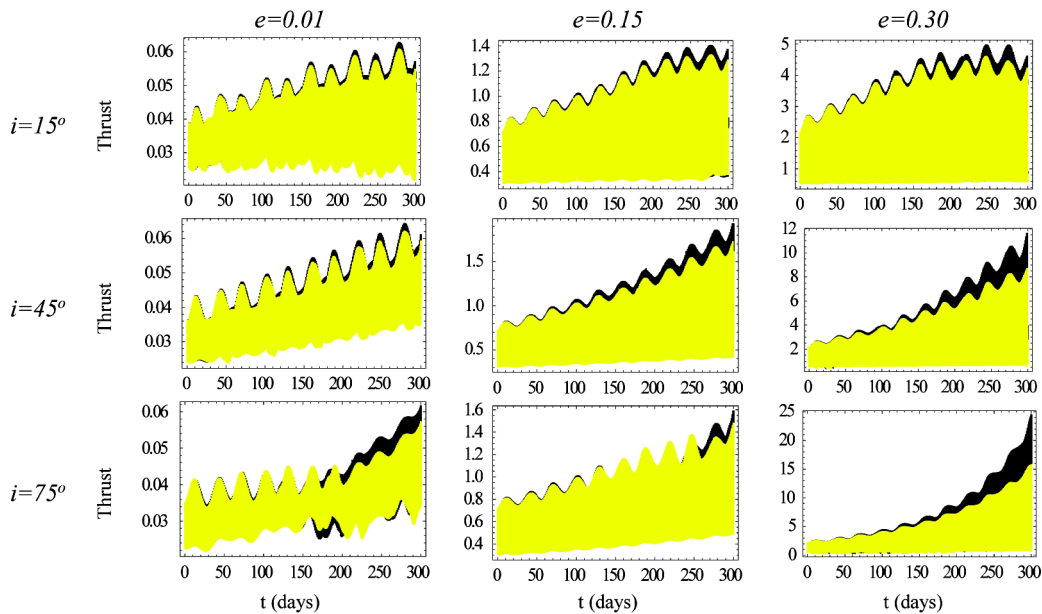


Fig. 9 Required thrust for in-track lunar formation keeping around different reference orbit eccentricity and inclination. (The yellow lines indicate the needed thrust with lunar obliquity and the black lines correspond to the results obtained neglecting the effect of the Moon's axial tilt.)

gument of perigee changes, the obliquity will be affected with a longer time. Also, in some cases the axial tilt effects cannot be ignored even with low flight time. Due to the above mentioned issues, consideration of the main-body's obliquity has a significant effect on the accuracy of formation flying.

4.3 The Effects of Orbital Elements and Obliquity on Formation Flying

Figure 8 shows the relative position of the follower satellite in relative coordinates LVLH, attached to the reference satellite. Also, the effects of different orbital elements of the reference satellite are investigated as well as obliquity effects. It should be noted that the orbital

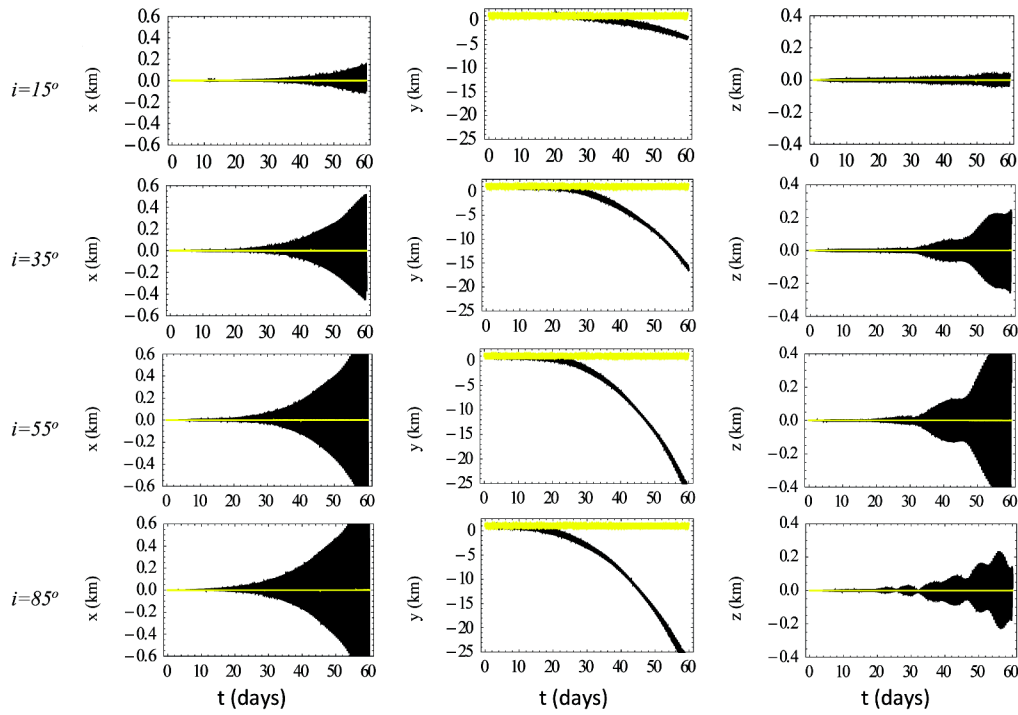


Fig. 10 The deviation of position from desired lunar in-track formation type due to neglect of lunar obliquity around the eccentricities and inclinations of different reference orbits. (Yellow and black correspond to simulation with and without consideration of lunar axial tilt, respectively.)

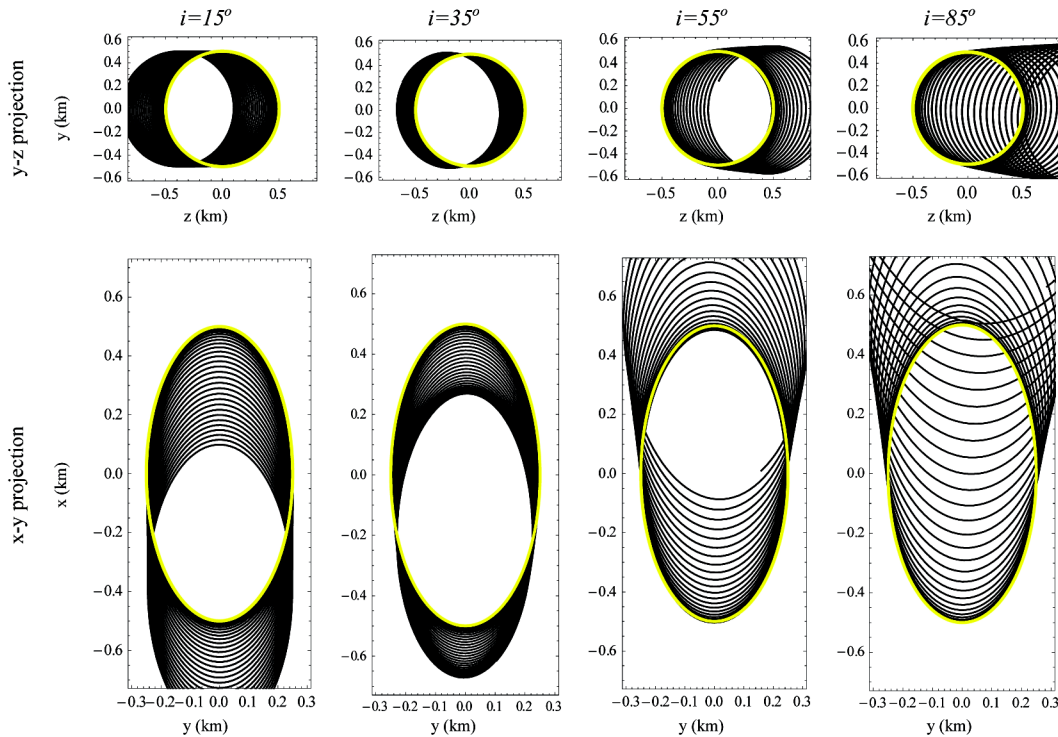


Fig. 11 The deviation from desired lunar PCO formation type due to neglect of the Moon’s axial tilt. (Yellow and black correspond to simulation with and without consideration of lunar obliquity, respectively.)

Table 1 The Initial Condition of a Follower Satellite in Different Scenarios due to Variations in Reference Satellite Orbital Elements

	$\delta\omega = 0.1^\circ$	$\delta\Omega = 0.1^\circ$	$\delta\theta = 0.1^\circ$	$\delta i = 0.1^\circ$
x (m)	0.7282	-7.7700	-7.282	-2.0021
y (m)	-2×10^{-10}	8626.5	9179.7	-3.4680
z (m)	-1.13×10^{-10}	-2717.7	0	4589.8
v_x (m s $^{-1}$)	-1.449	-14.676	-14.488	-0.0060
v_y (m s $^{-1}$)	-0.0012	-0.0126	-0.0126	-0.0104
v_z (m s $^{-1}$)	0	2.7294	0	13.802

elements of the reference and follower satellites are considered from Equation (59) (by applying the variation of $\delta\omega = 0.5^\circ$ for the follower satellite). As can be seen in Figure 8, the obliquity effect will show itself at a lower time, when the eccentricity increases. Also, with constant eccentricities and lower inclinations, the follower deviation will be considerable when ignoring the Moon's obliquity. Accordingly, consideration of the axial tilt effects is a crucial issue, specifically during long term flight.

4.4 The Obliquity Effects on Formation Flying Design

In this section the obliquity effects are investigated on formation flying design (Roscoe 2012; Roscoe et al. 2013). As presented in the previous sections, neglecting the obliquity in relative motion of satellites, a deviation is produced. The amount of this deviation has particular importance in design of a long-term formation flying mission. Here, two types of formation flying designs are investigated.

4.4.1 In-track formation design

One of the simplest methods of formation flying design is in-track formation. In this formation, the follower satellite moves in the orbital plane of the reference satellite with zero components except the along-track component (y) in the LVLH coordinate (Lane 2007). Here, we assume that

$$x_f(t) = z_f(t) = 0, \quad y_f(t) = \lambda \sin\left(\frac{2\pi}{T}t\right) + \zeta, \quad (60)$$

where x_f, y_f, z_f are the desired relative position components of the follower satellite and T is the period of the reference satellite orbit. With consideration of Equation (60), the follower satellite has a distance of $\zeta = 1$ km at perigee and $\zeta + \lambda = 1.5$ km at apogee in the case of in-track formation. Now, the required thrust for formation keeping and accomplishing the mission can be obtained by applying constraints in Equations (43)–(45). The amount of required thrust with and without considering the Moon's axial tilt has been shown in Figure 9. This necessary thrust is expressed in the following:

$$T_{xj} = -y_f \alpha_z - 2y_f \omega_z - \left(\frac{\mu}{r^3} + \frac{\mu'}{d^3}\right) + r'_x \mu' \left(\frac{1}{d^3} - \frac{1}{d_j^3}\right) + \left(\frac{\mu}{r_j^3} + \frac{\mu'}{d_j^3}\right) (r + x_j) + (\chi_j - \chi) s_\theta s_i + r (\gamma_j^2 - \gamma^2) \quad (61)$$

$$T_{yj} = -y_f (\omega_z^2 + \omega_x^2) + r'_y \mu' \left(\frac{1}{d^3} - \frac{1}{d_j^3}\right) + \left(\frac{\mu}{r_j^3} + \frac{\mu'}{d_j^3}\right) y_f + (\chi_j - \chi) s_\theta s_i \quad (62)$$

$$T_{zj} = y_f \alpha_x + 2y_f \omega_x + r'_z \mu' \left(\frac{1}{d^3} - \frac{1}{d_j^3}\right) + \left(\frac{\mu}{r_j^3} + \frac{\mu'}{d_j^3}\right) z_f + (\chi_j - \chi) c_i. \quad (63)$$

All parameters in Equations (61)–(63) have been introduced in previous sections. Also, in this case:

$$d_j = |\mathbf{r}' - \mathbf{r}_j| = \sqrt{(r'_x - r)^2 + (r'_y - y_f)^2 + r'_z{}^2} \quad (64)$$

$$r_j = \sqrt{r^2 + y_f^2}. \quad (65)$$

Figure 9 shows the effect of the Moon's obliquity on the thrust required for the mentioned in-track formation keeping. It is obvious that the obtained thrust is under the influence of the Moon's obliquity and it should not be ignored. In many former works, the effect of the main-body's obliquity has been disregarded in the investigation of a satellite's motion, but as has been demonstrated in (Liu et al. 2012), this parameter could play a significant role in the motion of a satellite over a long time.

As shown in Figure 10, the simulation of formation flying has been accomplished by solving the relative motion equation with regard to the above generated thrusts (Eqs. (61)–(63)), exclusively. When the obliquity effects are ignored, in the early time of the simulation, a large deviation occurs and the main goal of formation design fails. However, with consideration of the Moon's axial tilt in formation design, the formation is preserved in prolonged missions.

4.4.2 Projected Circular Orbit formation design

PCO formation flying is considered to further understand the importance of obliquity effects. This formation creates a circular image on the $z - y$ plane and motion of the follower satellite associated with this formation type in the LVLH coordinate (Yan et al. 2009) is assumed to be:

$$x_p(t) = 2\lambda \sin(nt + \alpha_0), \quad y_p(t) = \lambda \cos(nt + \alpha_0), \quad z_p(t) = \lambda \sin(nt + \alpha_0), \quad (66)$$

where $\alpha_0 = \pi/6$, $n = \sqrt{\mu/a^3}$ and λ is assumed equal to 0.5 km in this simulation. The required thrust for maintaining the formation characteristics can be procured with substitution of Equation (66) into Equations (43)–(45).

$$\begin{aligned} T_x = & -x_f (\omega_z^2 + n^2) - y_f \alpha_z + z_f \omega_z (2n + \omega_x) - r \frac{\mu'}{d^3} + r'_x \mu' \left(\frac{1}{d^3} - \frac{1}{d_j^3} \right) \\ & + \left(\frac{\mu}{r_j^3} + \frac{\mu'}{d_j^3} \right) (r + x_j) + (\chi_j - \chi) s_\theta s_i + r (\gamma_j^2 - \gamma^2) \end{aligned} \quad (67)$$

$$\begin{aligned} T_y = & -y_f (n^2 - n\omega_z + 2n\omega_x + \omega_z^2 + \omega_x^2) - x_f \alpha_z + z_f \alpha_x + r'_y \mu' \left(\frac{1}{d^3} - \frac{1}{d_j^3} \right) + \left(\frac{\mu}{r_j^3} + \frac{\mu'}{d_j^3} \right) y_j \\ & + (\chi_j - \chi) s_\theta s_i \end{aligned} \quad (68)$$

$$T_z = -z_f (n^2 + 2n\omega_x + \omega_x^2) + x_f \omega_x \omega_z + y_f \alpha_x + r'_z \mu' \left(\frac{1}{d^3} - \frac{1}{d_j^3} \right) + \left(\frac{\mu}{r_j^3} + \frac{\mu'}{d_j^3} \right) z_j + (\chi_j - \chi) c_i \quad (69)$$

where all parameters in Equations (67)–(69) were introduced in previous sections. Also, similar to the previous kind of formation, the generated thrust with and without consideration of the Moon's obliquity are obtained and applied in Equations (43)–(45) and (17)–(22) for analyzing motion of the follower satellite. When neglecting the Moon's obliquity, the $X - Y$ plane is taken as the third-body's (i.e. the Earth's) orbital plane instead of the equatorial plane of the Moon (it means that the third-body's inclination is ignored (Ren & Shan 2012)).

In Figure 11, deviation of satellite formation from the desired shape is shown for various scenarios due to neglecting effects of the Moon's axial tilt for different inclinations. Also, it can be seen that with consideration of the obliquity effects, formation is maintained even in prolonged operations.

5 CONCLUSIONS

In this paper, the near/far distance modeling of formation flying and analysis of relative motion were investigated by taking the third-body gravity and oblate main-body into account. The proposed model is based on new relative motion equations of satellites regarding a perturbing-body in an inclined orbit. In addition, the motion equations of the reference satellite were obtained without any simplifications by using a new approach that considers the third-body perturbation and axial tilt of the main-body. The suggested equations provide the possibility of considering the effects of the main-body's obliquity and oblateness on the relative motion model. In this work, the $X-Y$ plane was introduced as the equatorial plane of the main-body, not the third-body's orbital plane. After validating and comparing the motion equations of the reference satellite with previous works, the obtained relative motion equations have been validated against the MCRM equations that have been introduced in this paper. It was shown that neglecting obliquity causes a deviation in the follower satellite position, and this deviation is significant in prolonged missions.

Finally, for a further investigation of the effect of a third-body on formation missions, two kinds of formations (in-track and PCO) are introduced and the influence of axial tilt was studied. Accordingly, the obliquity of the main-body had a significant role in achieving long-term formation and future space missions.

References

- Alfriend, K. T., Vadali, S. R., Gurfil, P., How, J., & Breger, L. S. 2009, *Spacecraft Formation Flying: Dynamics, Control and Navigation* (Butterworth-Heinemann)
- Bertachini de Almeida Prado, A. F. 2003, *Journal of Guidance Control Dynamics*, 26, 33
- Bosanac, N., Howell, K. C., & Fischbach, E. 2016, *Ap&SS*, 361, 49
- Carvalho, J. P. S., Vilhena de Moraes, R., & Prado, A. F. B. A. 2010, *Celestial Mechanics and Dynamical Astronomy*, 108, 371
- Carvalho, J. P. d. S., de Moraes, R. V., & Prado, A. F. B. d. A. 2011, *Mathematical Problems in Engineering*, 2011
- Casotto, S. 2016, *Celestial Mechanics and Dynamical Astronomy*, 124, 215
- Chu, J., Guo, J., & Gill, E. K. A. 2015, *Celestial Mechanics and Dynamical Astronomy*, 121, 385
- Curtis, H. 2013, *Orbital Mechanics for Engineering Students* (Butterworth-Heinemann)
- Domingos, R., de Almeida Prado, A. B., & De Moraes, R. V. 2013, *Journal of Physics: Conference Series*, 465, 012017
- Domingos, R., Prado, A., & Gomes, V. 2014, *Mathematical Problems in Engineering*, 2014
- Domingos, R. d. C., Prado, A. D. A., & De Moraes, R. V. 2015, *Computational and Applied Mathematics*, 34, 507
- Feng, J., Nooten, R., Visser, P. N. A. M., & Yuan, J. 2015, *Ap&SS*, 357, 124
- Gaias, G., Ardaens, J.-S., & Montenbruck, O. 2015, *Celestial Mechanics and Dynamical Astronomy*, 123, 411
- Gomes, V. M., & de Cássia Domingos, R. 2015, *Computational and Applied Mathematics*, 1
- Gong, S., & Li, J. 2015, *Celestial Mechanics and Dynamical Astronomy*, 121, 121
- Gong, S., Li, J., & Baoyin, H. 2009, *Celestial Mechanics and Dynamical Astronomy*, 105, 159
- Gong, S., Yunfeng, G., & Li, J. 2011, *Acta Astronautica*, 68, 226
- Hu, Q., Zhang, Y., Zhang, J., & Hu, H. 2016, *Acta Astronautica*, 123, 446
- Kechichian, J. A. 1998, *The Journal of the Astronautical Sciences*, 46, 25
- Lane, C. M. 2007, *Formation Design and Relative Navigation in High Earth Orbits* (ProQuest)
- Lara, M., San-Juan, J. F., López, L. M., & Cefola, P. J. 2012, *Celestial Mechanics and Dynamical Astronomy*, 113, 435
- Liu, X., Baoyin, H., & Ma, X. 2012, *Ap&SS*, 339, 295
- Ma, X., & Li, J. 2013, *Ap&SS*, 348, 345
- Ortore, E., Cinelli, M., & Circi, C. 2016, *Celestial Mechanics and Dynamical Astronomy*, 124, 163
- Qi, Y., & Xu, S. 2015, *Ap&SS*, 359, 19
- Ren, Y., & Shan, J. 2012, *Celestial Mechanics and Dynamical Astronomy*, 114, 415
- Roscoe, C. W. T. 2012, *Satellite Formation Design in Orbits of High Eccentricity for Missions with Performance Criteria Specified Over a Region of Interest*, PhD Thesis, Texas A&M University
- Roscoe, C. W. T., Vadali, S. R., & Alfriend, K. T. 2013, *Journal of the Astronautical Sciences*, 60, 408
- Shahid, K., & Kumar, K. D. 2014, *Acta Astronautica*, 103, 269
- Tresaco, E., Elipe, A., & Carvalho, J. P. S. 2016, *Journal of Guidance, Control, and Dynamics*, 39, 1659
- Vallado, D. A. 2001, *Fundamentals of Astrodynamics and Applications* (CA: Microcosm Press; Dordrecht: Kluwer Academic Publishers)
- Wei, C., Park, S.-Y., & Park, C. 2013, *International Journal of Non Linear Mechanics*, 55, 55
- Xu, G., & Wang, D. 2008, *Journal of Guidance Control Dynamics*, 31, 1521
- Xu, G., Xiang, F., & Chen, Y. 2012, in *2012 24th Chinese Control and Decision Conference (CCDC)*, IEEE, 3676
- Yan, H., Alfriend, K. T., Vadali, S. R., & Sengupta, P. 2009, *Journal of Guidance Control Dynamics*, 32, 599
- Yang, H.-W., Zeng, X.-Y., & Baoyin, H. 2015, *RAA (Research in Astronomy and Astrophysics)*, 15, 1571
- Zeng, X.-Y., Jiang, F.-H., & Li, J.-F. 2015, *RAA (Research in Astronomy and Astrophysics)*, 15, 597